Formulation of Nanoparticles & Structural identification of 5-flurouacil for anti-cancer activity

Shweta Shukla[1], Satkar Prasad[2], Yogesh Pounikar[3]

1 Department of Pharmacy, PhD Research Scholar, Bhabha University Bhopal (M.P.)

2 Department of Pharmacy, Principal, Bhabha University, Bhopal (M.P.)

3 Department of Pharmacy, Professor & Principal, JK College of Pharmacy, Bilaspur (C.G)

Abstract

The objective of this study was to assess the effectiveness of 5-FU, a chemotherapy drug, in treating cancer. The drug was specifically targeted to the tumor cells using CAP nanoparticles with FA attached to them. A dispersion of 10-30 mg of FAC copolymer was created in 20 ml of acetone. A solution of 5- FU (30 mg) was dissolved in acetone and then slowly added to the prepared FAC solution. Pluronic F-68 (250 mg) was dissolved in distilled water to create solutions with different concentrations of Pluronic (1% and 2%). The particle size of FAC nanoparticles was determined using a particle size analyzer, and it was found to be 84±1.10 nm. The particle size distribution ranges from 84±1.10nm to 208±2.10nm due to the aggregation of particles. Based on the data presented in Table 1.2 increasing the amount of cellulose acetate phthalate (CAP-polymer) from 10 mg to 30 mg resulted in an increase in particle size from the range of 84 ±1.10 nm to 208 ±2.10 nm. The particle size range derived from CAP NPs ranged from 105±1.50 to 287±2.25 nm, as shown in Table 1.3. The polydispersity index (PDI) of FAC nanoparticles was determined to be 0.073 ± 0.05, while the PDI value of CAP nanoparticles was discovered to be 0.079 ± 0.10. The encapsulation efficiency of prepared FAC nanoparticles and CAP nanoparticles was found to be 93.65±1.15% and 90.50±1.15% respectively. The zeta potential of FAC nanoparticles was measured to be -13.1 mV, whereas for CAP nanoparticles it was discovered to be -5.98 mV (Table 1.4 and 7.4).

A nanoparticulate system composed of polymeric (CAP) materials. The FAC nanoparticles sustained the release of 5-FU for up to 48 hours, with a release rate of 98.52%. In contrast, normal CAP NPs released 97.5% of 5-FU within 12 hours. This is because the solvent system used in the manufacturing of the nanoparticle carrier, specifically acetone and isopropyl alcohol, can disrupt the hydrogen bond of FA. This disruption promotes the reaction between the carboxyl group of FA and the amine group of adipic acid dihydrazide through carbodiimide conjugation.

As a result, a cross-linked core-shell micelle is formed, which has lower solubility and facilitates sustained release. The hemolytic toxicity investigation was conducted to determine the hemotoxic effect of the designed FA attached cellulose acetate phthalate nanoparticle and plain cellulose acetate phthalate nanoparticles. The plain 5-FU, 5-FU loaded FAC NPs, and 5-FU loaded CAP NPs have shown hemolytic toxicity levels of 29.15±1.12%, 4.60±0.5%, and 8.65±1.05% respectively when tested in distilled water.

Keywords: Chemotherapy drug, Nanoparticles

Introduction: Cancer continues to be a significant cause of death and is a worldwide public health issue. Currently, chemotherapy is the most widely used treatment for cancer. However, its effectiveness is not ideal mostly because of the nonselective toxicity of the drugs used in chemotherapy. Therefore, the concept of cancer nanotechnology is proposed as a distinct method to

combat cancer by using nanotechnology in the treatment of cancer[1].

Historically, smoking has been the primary factor linked to the development of lung malignancies (U.S. Department of Health and Human Services, 2004). Conversely, lung cancer affects both those who smoke and those who do not smoke. For instance, the primary cause of around 65% of cancer-related deaths in women is lung cancer, mostly resulting from smoking, as opposed to other types of cancer such as breast, ovarian, and uterine cancer[2]. There is a lack of sufficient diagnostic and effective treatment procedures for lung cancer, such as chemotherapy, surgery, and radiation therapy.

5-FU is extensively utilized in the management of several types of malignancies, such as colorectal and breast tumors, as well as cancers affecting the aero digestive tract. When used alongside other chemotherapy drugs, 5-FU enhances response rates and increases survival in breast and While head and neck malignancies have been affected by 5-FU, it is in colorectal cancer where the drug has had the most significant influence. Chemotherapy using 5-FU has been shown to enhance both overall and disease-free survival rates in patients with surgically removed stage III colorectal cancer. However, the rate at which 5- FU-based chemotherapy effectively treats advanced colorectal cancer as the initial treatment is just 10-15%. The utilization of 5-FU in conjunction with more recent chemotherapies like IRINOTECAN and OXALIPLATIN has resulted in enhanced response rates for advanced colorectal cancer, reaching 40-50%. Nevertheless, in spite of these enhancements, there is an urgent want for novel therapeutic approaches[3].

2. Material & Methodology

Formation of FAC nanoparticles using FA-ADH-CAP Copolymer (FAC) and plain polymeric nanoparticles (CAP nanoparticle)

A dispersion of 10-30 mg of FAC copolymer was created in 20 ml of acetone. A solution of 5- FU (30 mg) was dissolved in acetone and then slowly added to the prepared FAC solution. Pluronic F-68 (250 mg) was dissolved in distilled water to create solutions with different concentrations of Pluronic (1% and 2%). The FAC solution was introduced into the pluronic solution while stirring continuously for a duration of 6 hours. The nanoparticles were subsequently separated using a membrane filter with a pore size of 0.45 μm and then subjected to centrifugation at a speed of 12,000 rpm for a duration of 10 minutes using a C-24, BL, Remi centrifuge from Mumbai, India. Following centrifugation, the supernatant was discarded and the FAC NPs were lyophilized for future use. Simple polymeric (CAP)

nanoparticles were synthesized using the previously described approach. The CAP NPs and FAC NPs were additionally freeze-dried and stored for future investigations.

Characterization parameters of FAC nanoparticles and CAP nanoparticle

2.1 Surface characteristics by Atomic force microscopy

The morphology and surface properties of the synthesized nanoparticles were analyzed using an Atomic Force Microscope (AFM) in contact mode, namely the SPM-9500 model manufactured by Shimadzu. The AFM analysis of the nanoparticles was conducted using a Si micro cantilever. The sample solution was applied onto mica and left undisturbed for one minute. The excess solution was then removed using compressed air. The resulting AFM photomicrograph was examined using SPM lab software.

2.2 Zeta potential & Particle size

The determination of the particle size and zeta potential of the formulated nanoparticles is performed using the Malvern equipment (DTS Ver. 60, Malvern Instruments, WR14 1XZ, UK). A suitably diluted mixture of CAP nanoparticles and FAC was introduced into the compartment of a particle size analyzer, yielding measurements for the average particle size and polydispersity index. The zeta potential, which represents the electric charge on the surface of a particle, is an indicator of the physical stability of a colloidal system. The zeta potentials of the FAC NPs and CAP NPs were determined using Laser Doppler Anemometry (LDA) with the Zeta sizer instrument from Malvern Instruments, UK.

2.3 DSC (Differential Scanning Calorimetry) analysis

The significant status of nanoparticles was determined by differential scanning calorimetry conducted with the DSC 60 instrument (Shimadzu, Kyoto, Japan). The 10mg samples (FA, 5- FU, Plain FAC, and 5FU loaded FAC NPs) were placed in an aluminum pan. The DSC thermogram was seen by scanning the temperature range up to 300°C at a heating rate of 10ºC/min under a nitrogen atmosphere.

2.4 XRD (X-Ray Diffraction)

X-Ray Diffractometry was used to analyze the crystalline properties of pure medicines, as well as the materials FA, polymer (CAP), and nanoparticle formulations, during the manufacturing of nanoparticles. The X-ray diffraction (XRD) patterns of powder samples (FA, 5-FU, FAC, and 5-FU loaded FAC NPs) were obtained using a Bruker AXS D8 Advance X-ray powder diffractometer.

2.5 Entrapment efficiency

5-FU anchored FAC NPs (10 mg) and CAP NPs (10 mg) were dispersed in an acetone solvent solution. Initially, the dispersion underwent centrifugation at a speed of 5000 revolutions per minute using a cooled centrifuge for approximately 15 minutes. This process aimed to separate and eliminate the polymeric debris, after which the liquid portion above the sediment, known as the supernatant, was collected. The transparentliquid portion of the solution was examined using High Performance Liquid Chromatography (HPLC) at a wavelength of 265 nm, specifically using the Wasters HPLC Model-515. This analysis was conducted to determine the quantity of 5- FU present in the nanoparticle system that was created, as described by Garg [3].

The HPLC system consists of the Wasters HPLC, Model 515, which includes an auto- sampler (Model 717 Plus), a column oven (Wasters CHM), and a PDA detector (Wasters 2998). Data collection and analysis were conducted using Empower version 2.0 software, developed by Milford, MA 01757 USA. The HPLC system typically consists of sensors with different wavelengths and a column (Zorbax C18, 250 × 4.60 mm, 5µ) that is used to evaluate 5-FU. The mobile phases employed were methanol and phosphate buffer with varying proportions (80:20 v/v), delivered at an optimal flow rate of 1 mL/min and maintained at a temperature of 55°C. Prior to usage, the mobile phase is degassed under vacuum (Venkataramana and Krishna, 1992)[4-5].

2.6 In-vitro drug release study

The drug (5-FU) loaded FAC nanoparticles and CAP nanoparticles were individually placed in separate dialysis bags (Himedia). These bags were then immersed in 50 ml of phosphate buffer saline (PBS) solution with a pH of 7.4. The solution was constantly stirred at 100 rpm at a temperature of 37±2°C. At regular intervals, 1ml of buffer solution was extracted and substituted with an equal volume of new buffer solution. The drug release from nanoparticles was quantified using a High Performance Liquid Chromatography (HPLC) system operating at a wavelength of 265 nm (Wasters HPLC, Model 515)[6-8].

Results

3.1 1H-NMR and FTIR spectroscopic analysis

The validation of the FAC copolymer was conducted using 1H-NMR and FTIR spectroscopy. Figure 7.1 displayed the spectroscopic curve of 1H-NMR and FTIR. The FTIR investigations yielded spectra ranging from 3600 cm-1 to 400 cm-1, as shown in Table 7.1. The FTIR spectra showed peaks at specific wavenumbers: 3250 cm-1 for the N-H stretch of amide, 2750 cm-1 and 1379 cm-1 for the presence of C-H alkene bond, 1732 cm-1 for the presence of C=O stretch, 1633 cm-1 indicating the formation of C=O bond, 1279 cm-1 for the C-N stretching of amide bond, and 1091 cm-1 for C=O stretching.The appearance of a characteristic peak at 3250 cm-1 and 1633 cm-1 verifies the existenceof an amide bond as well as a C=O carboxyl bond, indicating the formation of an amide bond between the amine group of ADH and both the carboxyl groups of FA and CAP. The 1H-NMR spectra of the FAC copolymer were depicted in Figure 7.2. The existence of FA, adipic acid dihydrazide (ADH), and cellulose acetate phthalate in FAC was verifiedby the appearance of unique peaks in the 1H NMR spectra. The FA proton was assigned at 2.5 ppm, while the cellulose acetate phthalate peak was observed between 1.6-2.0 ppm. The proton assignment for adipic acid dihydrazide (ADH) was found between 2.6-3.0 and 3.5 ppm. The inclusion of FA, adipic acid dihydrazide, and cellulose acetate phthalate in FAC copolymer is supported by the proton assignments. The conjugation and compatibility between FAC and cellulose acetate phthalate were confirmed through the execution of 1H-NMR and FTIR spectroscopic assays.

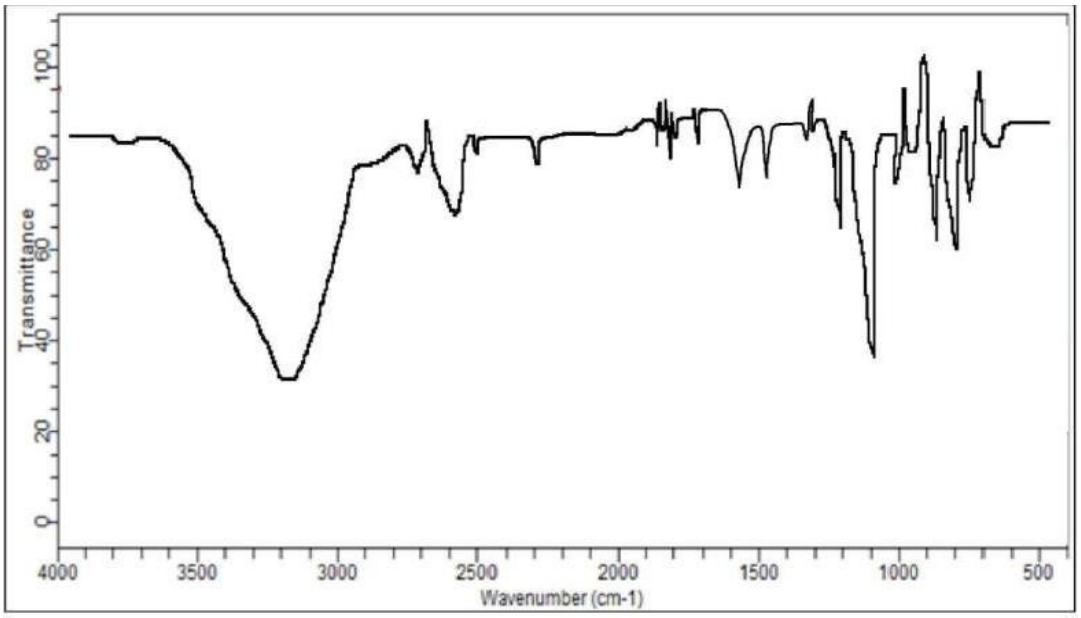

Fig. 1.1. FTIR spectrum of FAC copolymer

Table 1.1. FTIR interpretation of FAC nanoparticle

S.No.	Frequency of band (Cm^{-1})	Indication
1.	3250	N-H stretch of amide
2.	2750	C-H stretch
3.	1379	C-H stretch
4.	1732	C=O stretching
5.	1633	C=O stretching

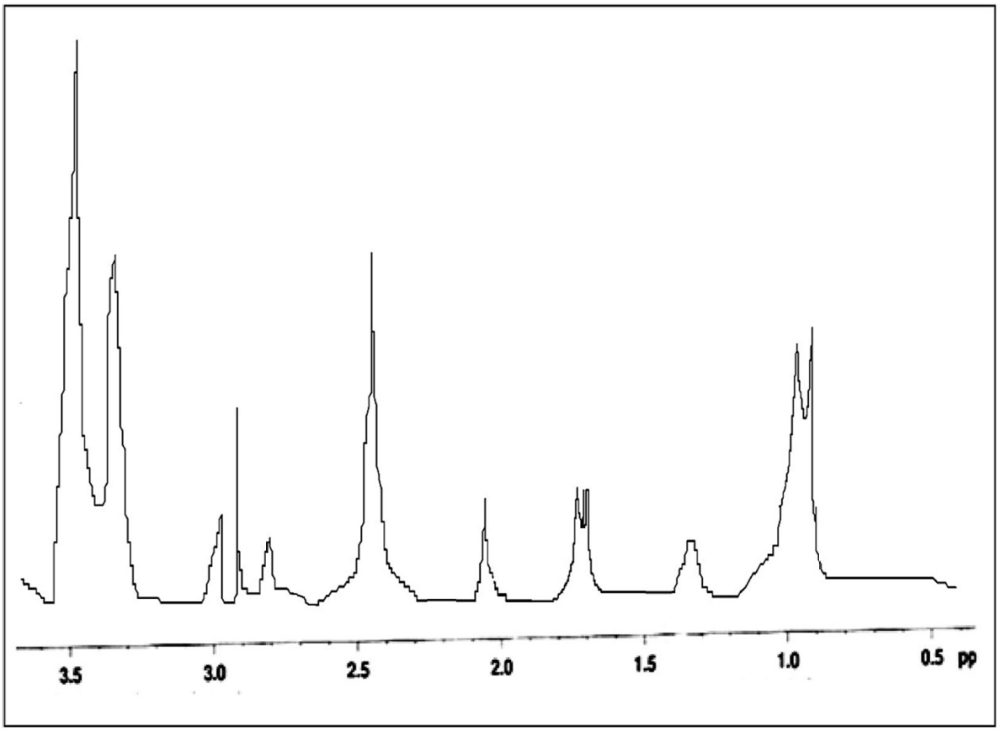

Fig. 1.2 NMR spectra of FAC copolymer

3.2 Surface Characteristics

The surface characteristics like shape, size and texture was examined by using atomic force microscopic technique (SPM-9500, Shimadzu).

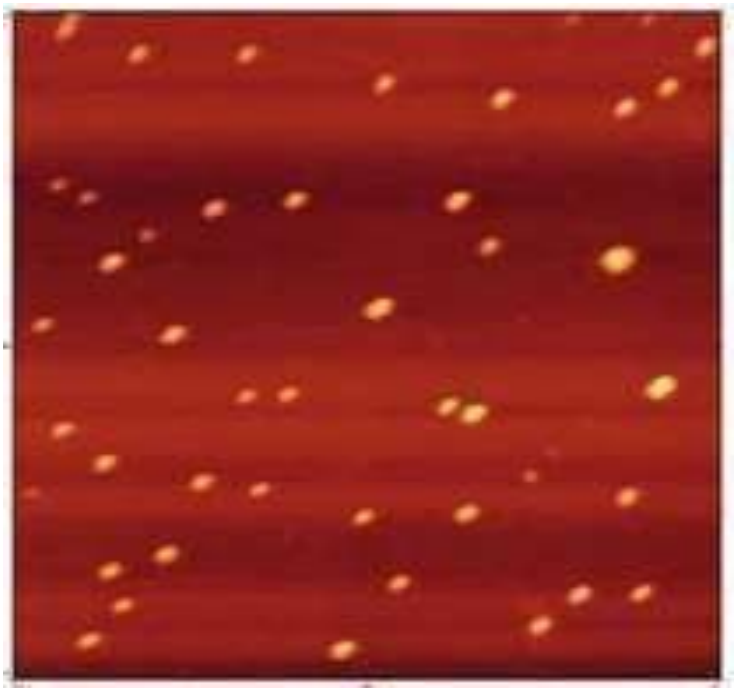

Fig.1.3. AFM image of FAC

The FAC nanoparticles, which were created, exhibited a spherical form and fell within the nanometric size range of 84-208 nm. This was confirmed by analyzing the single and 3D dimensions of the nanoparticles using AFM imaging (Fig. 7.3). The AFM examination yielded a photomicrograph displaying a consistent arrangement and homogeneous height of the nanoparticles. The results were expected to align with the prior findings [5].

3.3 Zeta Potential Determination, Particle Size analysis and Drug Entrapment Proficiency The particle size assessment of FAC nanoparticles was conducted using a particle size analyzer, revealing a particle size of FAC nanoparticles of 84±1.10 nm. The particle size distribution ranges from 84±1.10nm to 208±2.10nm due to the aggregation of particles. Based on the data presented in Table 7.2, increasing the amount of cellulose acetate phthalate (CAP-polymer) from 10mg to 30mg resulted in an increase in particle size from the range of 84±1.10nm to 208±2.10nm. The particle size range derived from CAP NPs ranged from 105±1.50 to 287±2.25nm, as shown in Table 7.3. The polydispersity index (PDI) of FAC nanoparticles was determined to be 0.073 ± 0.05, while the PDI value of CAP nanoparticles was measured to be 0.079 ± 0.10. The encapsulation efficiency of prepared FAC nanoparticles and CAP nanoparticles was found to be 93.65±1.15% and 90.50±1.15% respectively. The zeta potential of FAC nanoparticles was measured

to be - 13.1 mV, whereas for CAP nanoparticles it was discovered to be -5.98 mV (Table 7.4).

The entrapment efficiency of the drug nanoparticles was influenced by the concentration of surfactant and polymers, as demonstrated in the table. By increasing the amount of cellulose acetate phthalate (a type of polymer) from 10 mg to 30 mg, the size of FAC particles increases within the range of 84. The wavelength was reduced from 208nm to 93nm, resulting in a fall in entrapment efficiency of the medication from 93% to 72%. This loss in efficiency can be attributed to the increase in particle size. (Table 7.2) The polymer concentration had a comparable effect on CAP nanoparticles as it did on FAC NPs. The particle size increased from 105 nm to 287 nm as the amount of cellulose acetate phthalate(a polymer) was increased from 10 mg to 30 mg. The bigger size of particles and higher polymer content can negatively impact the encapsulation effectiveness of CAP nanoparticles, resulting in a reduction from 90% to 60% (Table 1.3). The surfactant concentration, namely Pluronic F-68, plays a crucial role in determining the particle size and drug entrapment effectiveness of FAC nanoparticles. Increasing the surfactant concentration

from 1% to 2% is likely to impact both the particle size and entrapment efficiency. When the concentration of surfactant was increased to 1%, the particle size decreased and there was an improvement in drug entrapment. However, when the concentration was further increased from 1% to 2%, the size of the nanoparticles increased due to particle aggregation, resulting in a decrease in the percentage of drug entrapped (Table 1.2). The polydispersity index (PDI) of FAC nanoparticles and CAP nanoparticles was determined to be 0.073±0.05 and 0.079±0.10, respectively. The PDI, or polydispersity index, is a dimensionless value that can vary within multiple ranges. Mono dispersed particles typically have a PDI index between 0.5 and 0.7. Samples with a wide range of particle sizes would have a PDI less than 0.7, as shown. The zeta potential of FAC and CAP was measured to be -13.1 mV and -5.98 mV correspondingly, as shown in Table 7.4. The negative zeta potential analysis of nanoparticles may be attributed to the presence of the carboxyl moiety in the polymer and the ligand. Charge particles with a high zeta potential result in the development of more stable structures. Particles experience increased repulsive contact. It was noted that a lower negative zeta potential can enhance the stability of the nanoparticle system.

Table 1.2 Ingredients and concentration using in the formulation of FAC nanoparticles.

S. No.	Drug: Polymer ratio (mg)	Internal phase			External phase		% Entrapment efficiency	Particle size (nm)
		5-FU (mg)	FAC (mg)	Acetone (ml)	Pluronic F-68 (mg)	Water (ml)		
S1	30:10	30	10	20	250	25	74.50±1.50	197±1.15
S2	30:20	30	20	20	250	25	80.11±1.15	139±0.50
S3	30:30	30	30	20	250	25	93.65±1.15	84±1.10
S4	30:10	30	10	20	500	25	72.61±0.75	208±2.10
S5	30:20	30	20	20	500	25	78.32±0.75	165±1.15
S6	30:30	30	30	20	500	25	85.45±0.50	117±1.50

S: Sample, 5-FU: 5-Fluorouracil

Table 1.3 Ingredients and concentration using in the formulation of CAP nanoparticles.

S. No.	Drug: Polymer ratio (mg)	Internal phase			External phase		% Entrapment efficiency	Particle size(nm)
		5-FU (mg)	CAP (mg)	Acetone (ml)	Pluronic F-68(mg)	Water (ml)		
S1	30:10	30	10	20	250	25	64.25±1.50	258±0.50
S2	30:20	30	20	20	250	25	74.50±0.50	199±0.15
S3	30:30	30	30	20	250	25	90.50±1.15	105±1.50
S4	30:10	30	10	20	500	25	60.15±0.50	287±2.25
S5	30:20	30	20	20	500	25	68.21±1.75	235±1.17
S6	30:30	30	30	20	500	25	80.20±0.25	142±1.15

S: Sample, 5-FU: 5-Fluorouracil

Table 1.4 Optimum particle size &entrapment efficiency of FAC and CAP nanoparticles.

S. No.	Formulations	Entrapment efficiency	Particle size (nm)	Polydispersity Index	Zeta Potential
1.	FAC NPs	93.65±1.15	84±1.10	0.0732±0.05	-13.1 mV
2.	CAP NPs	90.50±1.15	105±1.50	0.079±0.10	-5.98 mV

3.4 Differential scanning calorimetry (DSC) analysis

Differential scanning calorimetry (DSC) thermograms of FA, 5-FU, FAC NPs, and 5-FU loaded FAC NPs were obtained and presented in Figure 1.4. A significant endothermic peak of FA was observed at 245ºC, indicating its unique characteristic. A peak with endothermic properties was seen at a temperature of 284ºC for 5-FU. An endothermic peak at 245ºC was observed while analyzing the drug-free FAC NPs. The drug loaded nanoparticle (5-FU-FAC NPs) exhibited an endothermic peak of FA at 250ºC, while the endothermic peak of 5-FU at 280- 282ºC indicated its presence in the nanoparticles. The DSC analysis revealed that the exothermic peak of 5-FU in the thermogram of 5-FU loaded FAC NPs occurred at 282ºC. This indicates that 5-FU is present in a crystal-like form within the nanoparticle micelle.

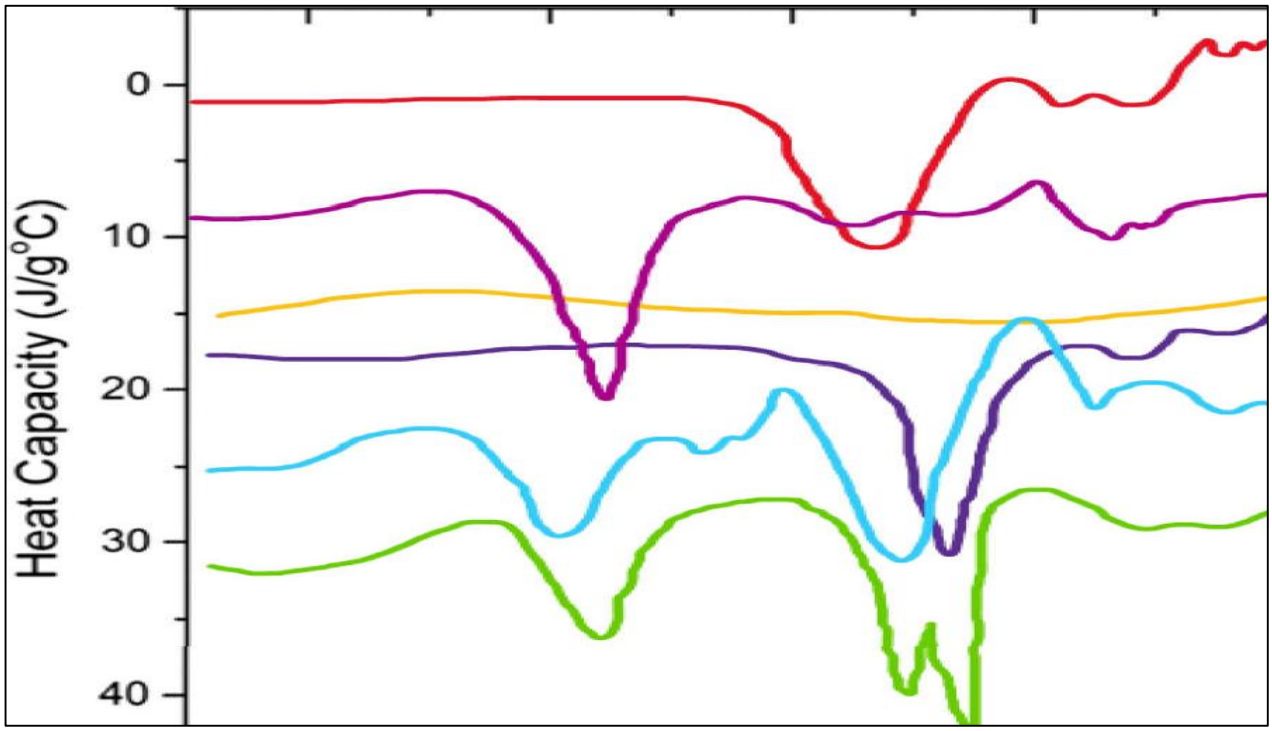

Fig.1.4. DSC thermogram: (a) FA;(b) ADH; (c) CAP; (d) 5-FU; (e) FAC (without5-FU); (5) FAC (with 5-FU).

3.5 Powder X-Ray diffraction investigation

The X-ray diffraction (XRD) patterns of FA, 5-FU, FAC NPs, and 5-FU loaded FACNPs are described in Figure 7.5. For the case of FA, the X-ray diffract gram exhibited a prominent peak within the 2θ range of 10 to 32. At angles of 15°, 22°, 24°, 29°, and32°, little sharp peaks were seen, indicating the crystalline nature of FA. The medication 5-FU has distinct and well- defined peaks at 8, 15, 16, 21, 23, 27, and 30, confirming its crystalline nature.

The diffractogram of FAC has peaks at 15, 24, 28, 32, and 33θ. The presence of distinctive crystalline peaks at 8, 10, 15, 18, 23, 27, 30, 32, and 33θ in the 5-FU loadedFAC NPs

indicates an increase in crystallinity. “This suggests that 5-FU is mixed withits crystalline form, as seen in Figure 7.5 (f). The XRD diffractogram revealed the presence of multiple diffracto grams of 5-FU in the 5-FU loaded FAC NPs. This indicates that the 5-FU loaded FAC NPs are suitable for regulated and sustained drug release from the nanoparticle system”.

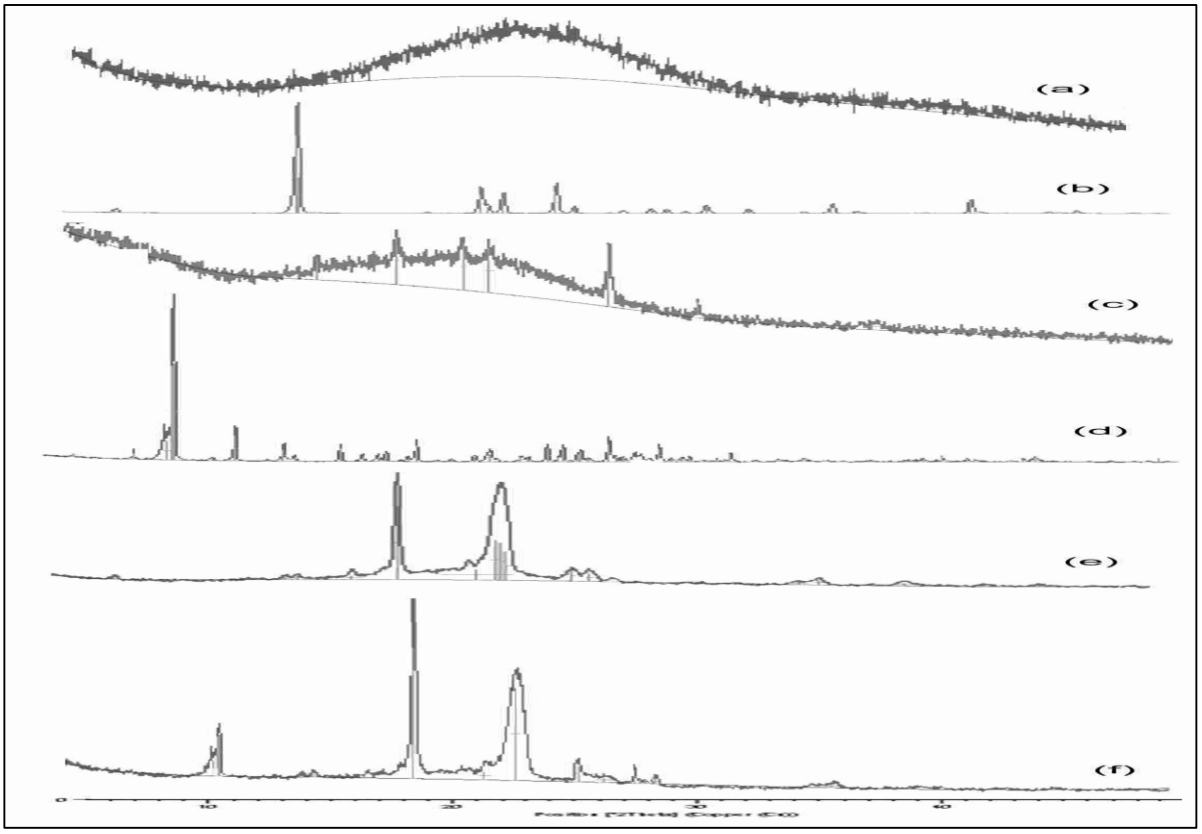

Fig. 1.5. XRD thermo gram: (a) FA; (b) ADH; (c) CAP; (d) 5-FU; (e) FAC(without 5-FU); (e) FAC (with 5-FU).

Summary & Conclusion:

The objective of this study was to assess the effectiveness of 5-FU, a chemotherapy drug, in treating cancer. The drug was specifically targeted to the tumor cells using CAP nanoparticles with FA attached to them.

The validation of the FAC copolymer was conducted using 1H-NMR and FTIR spectroscopy. Figure 1.1 displayed the spectroscopic curve of 1H-NMR and FTIR. The FTIR investigations yielded spectra ranging from 3600 cm-1 to 400 cm-1, as shown in Table 1.1. The FTIR spectra showed peaks at specific wavenumbers: 3250 cm-1, indicating the N-H stretch of amide; 2750 cm-1 and 1379 cm-1, indicating the presence of C-H alkene bond; 1732 cm-1, indicating the presence of C=O stretch; 1633 cm-1, indicating the formation of C=O bond; 1279 cm-1, indicating the C-N stretching of amide bond; and 1091 cm-1, indicating C=O stretching. The appearance of a characteristic peak at 3250 cm-1 and 1633 cm-1 verifies the existence of an amide bond as well as a C=O carboxyl bond, indicating the formation of an amide bond between the amine group of ADH and both the carboxyl groups of FA and CAP.

The 1H-NMR spectra of the FAC copolymer were depicted in Figure 1.2. The existence of FA, adipic acid dihydrazide (ADH), and cellulose acetate phthalate in FAC was verified by the appearance of unique peaks in the 1H NMR spectra. The FA proton was assigned at 2.5 ppm, while the cellulose acetate phthalate peak was observed between 1.6-2.0 ppm. The proton assignment for adipic acid dihydrazide (ADH) was found between 2.6-3.0 and 3.5 ppm. The inclusion of FA, adipic acid dihydrazide, and cellulose acetate phthalate in the FAC copolymer is supported by the proton assignments. The conjugation and compatibility between FAC and cellulose acetate phthalate were confirmed using 1H- NMR and FTIR spectroscopic assays.

The atomic force microscopic technique (SPM-9500, Shimadzu) was used to assess the surface properties, including shape, size, and roughness. The FAC nanoparticles were spherical in shape and had a nano metric size range of 84- 208 nm, as observed in the AFM picture for both single and 3D dimensions (Fig. 7.3). The AFM examination yielded a photomicrograph displaying a consistent arrangement and homogeneous height of the nanoparticles. The results were expected to align with the prior findings [9].

The particle size of FAC nanoparticles was determined using a particle size analyzer, and it was found to be 84±1.10 nm. The particle size distribution ranges from 84±1.10nm to 208±2.10nm due to the aggregation of particles. Based on the data presented in Table 1.2 increasing the amount of cellulose acetate phthalate (CAP-polymer) from 10 mg to 30 mg resulted in an increase in particle size from the range of 84 ± 1.10 nm to 208 ±2.10 nm. The particle size range derived from CAP NPs ranged from 105±1.50 to 287±2.25 nm, as shown in Table 1.3. The polydispersity index (PDI) of FAC nanoparticles was determined to be 0.073 ± 0.05, while the PDI value of CAP nanoparticles was discovered to be 0.079 ± 0.10. The encapsulation efficiency of prepared FAC nanoparticles and CAP nanoparticles was found to be 93.65±1.15% and 90.50±1.15% respectively. The zeta potential of FAC nanoparticles was measured to be -13.1 mV, whereas for CAP nanoparticles it was discovered to be -5.98 mV (Table 1.4 and 7.4).

The table1.4 results show that the entrapment efficiency of the drug nanoparticles was influenced by the concentration of surfactant and polymers, which in turn affected the size of the particles. By increasing the amount of cellulose acetate phthalate (a type of polymer) from 10 mg to 30 mg, the size of FAC particles increased from the range of 84nm to 208 nm. However, this increase in particle size led to a decrease in entrapment effectiveness of the drug content, from a range of 93% to 72%. Therefore, the efficiency of the process was affected by the increase in particle size.

The occurrence of entrapment may be reduced (Table 1.2). The polymer concentration had a comparable impact on CAP nanoparticles as it did on FAC NPs. The particle size increased from 105 nm to 287 nm as the amount of cellulose acetate phthalate (a polymer) was increased from 10 mg to 30 mg. The bigger size of particles and higher polymer content can negatively impact the encapsulation effectiveness of CAP nanoparticles, resulting in a reduction from 90% to 60% (Table 1.3). The surfactant concentration (pluronic F-68) has a key effect in determining the particle size and percentage drug entrapment efficiency of FAC nanoparticles. Increasing the surfactant concentration from 1% to 2% may also influence the particle size and entrapment efficiency. When the concentration of surfactant was increased to 1%, the particle size decreased and there was an improvement in drug entrapment. However, when the concentration was further increased from 1% to 2%, the size of the nanoparticles increased due to particle aggregation, resulting in a decrease in the percentage of drug entrapped (Table 1.2). The polydispersity index (PDI) of FAC nanoparticles and CAP nanoparticles was determined to be 0.073±0.05 and 0.079±0.10, respectively. PDI, or Polydispersity Index, is a dimension less value that varies within distinct ranges. For mono dispersed particles, the PDI index falls between 0.5 and 0.7. Samples with a wide range of particle sizes have a PDI value less than 0.7.

The occurrence of entrapment may be reduced (Table 1.2). The polymer concentration had a comparable impact on CAP nanoparticles as it did on FAC NPs. The particle size increased from 105 nm to 287 nm as the amount of cellulose acetate phthalate (a polymer) was increased from 10 mg to 30 mg. The bigger size of particles and higher polymer content can negatively impact the encapsulation effectiveness of CAP nanoparticles, resulting in a reduction from 90% to 60% (Table 1.3). The surfactant concentration (pluronic F-68) has a key effect in determining the particle size and percentage drug entrapment efficiency of FAC nanoparticles. Increasing the surfactant concentration from 1% to 2% may also influence the particle size and entrapment efficiency. When the concentration of surfactant was increased to 1%, the particle size decreased and there was an improvement in drug entrapment. However, when the concentration was further increased from 1% to 2%, the size of the nanoparticles increased due to particle aggregation, resulting in a decrease in the percentage of drug entrapped (Table 1.2). The polydispersity index (PDI) of FAC nanoparticles and CAP nanoparticles was determined to be 0.073±0.05 and 0.079±0.10, respectively. PDI, or Polydispersity Index, is a dimension less value that varies within distinct ranges. For mono dispersed particles, the PDI index falls between 0.5 and 0.7. Samples with a wide range of particle sizes have a PDI value less than 0.7.as shown[6].The Zeta potential of FAC and CAP was measured to

be -13.1 mV and -5.98 mV correspondingly, as shown in Table 1.4.The negative zeta potential analysis of nanoparticles may be attributed to the presence of the carboxyl moiety in the polymer and the ligand.

Differential scanning Calorimetry (DSC) was used to obtain and present thermo grams of FA, 5-FU, FAC NPs, and 5-FU loaded FAC NPs (Figure 1.4). A significant endothermic peak of FA was observed at 245ºC, indicating its unique thermal behavior. The temperature at which the endothermic peak of 5-FU was observed was 284ºC. An endothermic peak at 245ºC was observed while analyzing the drug-free FAC NPs. The drug loaded nanoparticle (5-FU-FAC NPs) exhibited an endothermic peak of FA at 250ºC, while the endothermic peak of 5-FU at 280- 282ºC indicated its presence in the nanoparticles. The DSC analysis revealed that the 5-FU loaded FAC NPs exhibited an exothermic peak at 282ºC in the thermo gram. This peak indicates that the 5-FU is present in a crystalline state within the nanoparticle micelle.

The X-ray diffraction (XRD) patterns of FA, 5-FU, FAC NPs, and 5-FU loaded FAC NPs are described in Figure 1.5. For the case of FA, the X-ray diffract gram exhibited a prominent peak within the 2θ range of 10 to 32. At angles of 15°, 22°, 24°, 29°, and 32°, little sharp peaks were seen, indicating the crystalline nature of FA. The medication 5-FU has distinct and well- defined peaks at 8, 15, 16, 21, 23, 27, and 30, confirming its crystalline nature. The diffracto gram of FAC has peaks at 15, 24, 28, 32, and 33θ. The presence of distinctive crystalline peaks at 8, 10, 15, 18, 23, 27, 30, 32, and 33θ in the 5-FU loaded FAC NPs indicates an increase in crystallinity. This suggests that 5-FU is mixed with its crystalline form, as seen in Figure 1.5 (f). The XRD diffracto gram revealed the presence of multiple diffract grams of 5-FU in the 5-FU loaded FAC NPs. It is now understood that these nanoparticles are well-suited for regulated and extended drug release.

The graph (Fig. 1.6, Table 1.5) demonstrates the extended and continuous release of the medication from the nanoparticle system. The drug release graph illustrates the controlled and sustained release of 5-FU from both the FAC system and the simple system. A nanoparticulate system composed of polymeric (CAP) materials. The FAC nanoparticles sustained the release of 5-FU for up to 48 hours, with a release rate of 98.52%. In contrast, normal CAP NPs released 97.5% of 5-FU within 12 hours. This is because the solvent system used in the manufacturing of the nanoparticle carrier, specifically acetone and isopropyl alcohol, can disrupt the hydrogen bond of FA. This disruption promotes the reaction between the carboxyl group of FA and the amine group of adipic acid dihydrazide through carbodiimide conjugation.

As a result, a crosslinked core-shell micelle is formed, which has lower solubility and facilitates sustained release. The hemolytic toxicity investigation was conducted to determine the hemotoxic effect of the designed FA attached cellulose acetate phthalate nanoparticle and plain cellulose acetate phthalate nanoparticles. The plain 5-FU, 5-FU loaded FAC NPs, and 5-FU loaded CAP NPs have shown hemolytic toxicity levels of 29.15±1.12%, 4.60±0.5%, and 8.65±1.05% respectively when tested in distilled water. These results are presented in Table 1.6. The plain 5-FU and 5-FU loaded nanoparticle formulations had 0.1μM equivalents of 5-FU. The efficacy of the 5-FU nanoparticle formulation was assessed based on the drug content. The delayed release of encapsulated drug molecules in the nanoparticles resulted in a reduction in hemolytic toxicity. The results from the hemolytic toxicity investigation showed that the 5-FU containing FAC NPs had lower hemotoxicity compared to the 5-FU loaded CAP NPs. This could be attributed to the hydrophilic properties of FA, which contribute to the development of a hemocompatible system. The suppression of hemotoxicity caused by the medication can be associated with other research on nanoparticles that have been previously published As a result, a crosslinked core-shell micelle is formed, which has lower solubility and facilitates sustained release. The hemolytic toxicity investigation was conducted to determine the hemotoxic effect of the designed FA attached cellulose acetate phthalate nanoparticle and plain cellulose acetate phthalate nanoparticles. The plain 5-FU, 5-FU loaded FAC NPs, and 5-FU loaded CAP NPs have shown hemolytic toxicity levels of 29.15±1.12%, 4.60±0.5%, and 8.65±1.05% respectively when tested in distilled water. These results are presented in Table 1.6. The plain 5-FU and 5-FU loaded nanoparticle formulations had 0.1μM equivalents of 5-FU. The efficacy of the 5-FU nanoparticle formulation was assessed based on the drug content. The delayed release of encapsulated drug molecules in the nanoparticles resulted in a reduction in hemolytic toxicity. The results from the hemolytic toxicity investigation showed that the 5-FU containing FAC NPs had lower hemotoxicity compared to the 5-FU loaded CAP NPs. This could be attributed to the hydrophilic properties of FA, which contribute to the development of a hemocompatible system. The suppression of hemotoxicity caused by the medication can be associated with other research on nanoparticles that have been previously published [10].

Reference

1. Jones, D. (2007). Cancer nanotechnology: small, but heading for the big time. *Nature Reviews Drug Discovery*, *6*(3), 174-175. doi:10.1038/nrd2285.

2. Mukerjee, A., & Vishwanatha, J.K.(2009). Formulation, characterization and evaluation of curcumin-loaded plga nanospheres for cancer therapy. *Anticancer Research*, 29(10), 3867-75.

3. Müller, K.C. (2001) Pharmaceutically relevant metabolites from lichens. *Applied Microbiology and Biotechnology*, *56*(1-2), 9-16. doi:10.1007/s002530100684.

4. Nidhin, M., Indumathy, R., Sreeram, K. J., & Nair, B. U. (2008). Synthesis of iron oxide nano-particles of narrow size distribution on polysaccharide templates. *Bulletin of Materials Science*, *31*(1), 93-96. doi:10.1007/s12034-008-0016-2.

5. Rodriguez, E., & Lilenbaum, R. C. (2010). Small Cell Lung Cancer: Past, Present, and Future. *Current Oncology Reports*, *12*(5), 327-334. doi:10.1007/s11912-010-0120-5.\

6. Garg, A., Rai, G., Lodhi, S., Jain, A.P., & Yadav, A.K. (2014). *In-vitro* and *in-vivo* assessment of dextran-appended cellulose acetate phthalate nanoparticles for transdermal delivery of 5- fluorouracil. *Drug Delivery*, 1-11. doi:10.3109/10717544.2014.978512.

7. Companella, L.,Delfini, M.,Ercole, P.,lacoangeli, A., & Risuleo, G.(2002). Molecular characterization and action of usinic acid; a drug that inhibits proliferation of mouse polyomavirus in vitro and whose main target is RNA transcription. Biochimie, 84(4), 329-334. Doi:10.1016/s0300-9084

8. Budhian, A., Siegel, S.J., & Winey, K.l. (2008) Controlling the in vitro release profiles for a system of haloperidol-loaded PLGA nanoparticles, International Journal of Pharmaceutics, 346 (1-2),l 151-159. Doi;10.1002/(sici) 1097-4628 (19970103) 63:1.

9. Calvo, P., Remunan-Lopez, C., Vila-jatao, J.L.,& Alaanso, M.J. 1997). Chitosan & Chitosan/Ethylene oxide-propylene Oxide Block Co-polymer Nanoparticles as Novel Carriers for Proteins and Vaccines, Pharmaceutical Research, 14(10), 1431-1436. doi; 10.1023/a;1023/a;10121 28907255.

10. Garg, A., Rai, G., Lodhi, S., Jain, A. P., & Yadav, A. K. (2016). Hyaluronic acid embedded cellulose acetate phthalate core/shell nanoparticulate carrier of 5-fluorouracil. *International Journal of Biological Macromolecules*, *87*, 449- 459. doi:10.1016/j.ijbiomac.2015.11.094.